Volume 10
Number 19
7 October 2020
Pages 6395–6742

Catalysis Science & Technology

rsc.li/catalysis

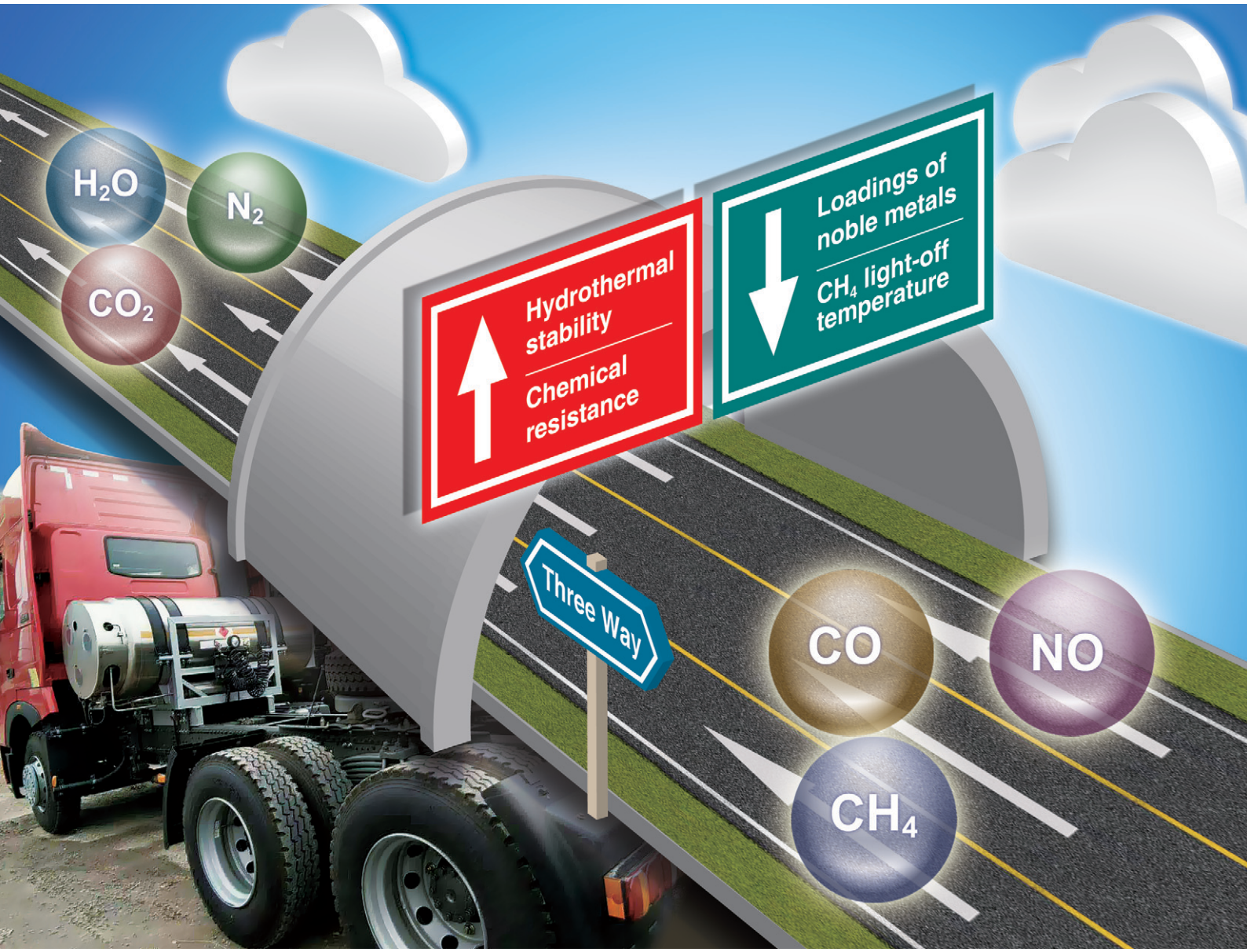

ISSN 2044-4761

ROYAL SOCIETY OF CHEMISTRY

MINIREVIEW
Wenpo Shan, Yan Zhang *et al.*
Recent advances in three-way catalysts of natural gas vehicles

Catalysis Science & Technology

ROYAL SOCIETY OF CHEMISTRY

MINI REVIEW

View Article Online
View Journal | View Issue

Check for updates

Cite this: *Catal. Sci. Technol.*, 2020, **10**, 6407

Recent advances in three-way catalysts of natural gas vehicles

Cenyan Huang,[ab] Wenpo Shan, *[ab] Zhihua Lian, [a] Yan Zhang*[ab] and Hong He[acd]

Received 1st July 2020,
Accepted 4th August 2020

DOI: 10.1039/d0cy01320j

rsc.li/catalysis

Natural gas vehicles (NGVs), as alternatives to gasoline and diesel vehicles, have been rapidly and widely promoted in the past 20 years. The three-way catalyst (TWC) technology is one of the dominant technologies for gaseous emission control of NGVs. However, it is still a great challenge to purify the exhaust gas of NGVs to meet increasingly strict emission limits, particularly for CH_4 and NO_x. This review is focused on the recent research advances in TWCs for NGVs, including the technical fundamentals, classic components (active phases, supports, and promoters), novel preparations of catalysts, resistance to thermal and chemical aging, current challenges and future perspectives. Particular attention is given to Pd-based catalysts as typical commercial TWCs, and potential alternatives which have competitive three-way catalytic performance are also highlighted.

Published on 05 August 2020. Downloaded on 11/17/2020 7:25:32 AM.

1. Introduction

With the increasing shortage of global petroleum resources and rising oil prices, natural gas vehicles (NGVs), as alternatives to gasoline and diesel vehicles, have been rapidly and widely promoted both in the passenger and commercial vehicle markets due to the advantages of abundance, low price, little environmental impact, and high compatibility.[1–3] At the end of November 2018, the number of global NGVs had exceeded 26 million (only after gasoline vehicles and diesel vehicles).[4] Due to their vigorous growth, NGVs are anticipated to contribute more than 7% (only after electric vehicles) of the global commercial vehicle market in 2040.[5] On the other hand, affected by government policies, natural gas resources and prices, the worldwide development of NGVs is extremely unbalanced. By November 2018, the amount of NGVs in Asia-Pacific accounted for around 70.0% of the global total (Fig. 1). Among all the countries surveyed, China has become the world's largest NGV market with more than 6 million vehicles and 8400 natural gas stations in 2018.[4]

Although NGVs have obtained a remarkable growth worldwide, the fundamental understanding of their real-world emissions is very limited. According to previous studies, exhaust emissions from NGVs which were equipped with three-way catalysts (TWCs) might still exceed emission limits, in particular for hydrocarbon compounds (HCs) and NO_x (Table 1).[6–9] Since the conventional control technologies for NGVs hardly meet emission limits, their exhaust pollution should be paid high attention. In addition, the emission limits of NGVs have become stricter both in developed and developing countries (Table 2). The Euro 6 standard requires a 50% decrease for CH_4 and NO_x emissions compared with Euro 5.[10,11] Starting from 2020, the China 6 standard requires even stricter limits for light-duty vehicles than the Euro

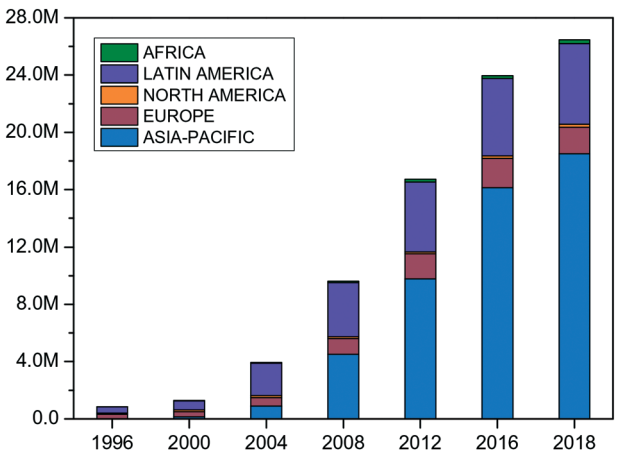

Fig. 1 Global development of NGVs from 1996 to 2018.[4]

[a] *Center for Excellence in Regional Atmospheric Environment and Key Laboratory of Urban Pollutant Conversion, Institute of Urban Environment, Institute of Urban Environment, Chinese Academy of Sciences, Xiamen 361021, China. E-mail: wpshan@iue.ac.cn, yzhang3@iue.ac.cn*
[b] *Zhejiang Key Laboratory of Urban Environmental Processes and Pollution Control, Ningbo Urban Environment Observation and Research Station, Chinese Academy of Sciences, Ningbo 315800, China*
[c] *State Key Joint Laboratory of Environment Simulation and Pollution Control, Research Center for Eco-Environmental Sciences, Chinese Academy of Sciences, Beijing 100085, China*
[d] *University of Chinese Academy of Sciences, Beijing 100049, China*

Published on 05 August 2020. Downloaded on 11/17/2020 7:25:32 AM.

Table 1 Emissions from NGVs equipped with TWCs in previous studies

Type	Engine	Standard	Test condition	Avg. speed (km h^{-1})	CO (g km^{-1})	HC (g km^{-1})	CH_4 (g km^{-1})	NO_x (g km^{-1})	Ref.
Taxi	Four-cylinder engine with bi-fuel system	Euro 2	Urban roads and a highway	40.7	1.0 ± 1.1 (2.2[a])	1.37 ± 0.53 (0.5[a])	—	2.13 ± 0.77 (0.5[a])	6
		Euro 3		39.5	0.6 ± 0.5 (2.3[b])	0.61 ± 0.39 (0.2[b])	—	1.19 ± 1.27 (0.15[b])	6
Truck	Otto 7790cc CNG engine	—	A closed track	8.16	15.8	2.19	—	4.38	7
Truck	Stoichiometric natural gas engine	—	Urban roads	—	7.53 ± 0.72 (g mi^{-1})	0.032 ± 0.026 (NMHC) (g mi^{-1})	—	0.579 ± 0.077 (g mi^{-1})	8
Station wagon and van	1.4 TSI with CNG (gasoline) system	Euro 6	Urban route cold start	18.3	0.149 (2.27[c])	0.193 (0.108[c])	0.035	0.048 (0.082[c])	9
		Euro 6	Urban route hot start	23.4	0.108	0.165	0.045	0.063	9
		Euro 6	Mixed route	58.2	0.112	0.149	0.018	0.186	9

[a] For Euro 2 standard. [b] For Euro 3 standard. [c] For Euro 6 standard.

Table 2 Emission standards for diesel and gas engines of heavy-duty vehicles (g kW^{-1} h^{-1}) and gasoline and gas engines of light-duty vehicles (g km^{-1})

Type	Weight (kg)	Standard	Date	Test	CO	THC	NMHC	CH_4[a]	NO_x	NO_x + NMHC
Heavy-duty	>3500	Japan 2009	2009	WHTC	2.22	0.17	—	—	0.40	—
	>2610	Euro 6	2013	WHTC	4.0	—	0.16	0.50	0.46	—
	>3500	China 6	2020	WHTC	4.0	—	0.16	0.50	0.46	—
	>8500 (lbs)	EPA 2007	2007	FTP	—	—	0.14 (g per bhp h)		0.20 (g per bhp h)	—
Light-duty	<3500	Japan 2009	2009	WLTP	1.92	—	0.08	—	0.08	—
	<2610	Euro 6	2014[b] (2015[c])	NEDC	1.0[b] (2.27[c])	0.10[b] (0.16[c])	0.068[b] (0.108[c])	—	0.06[b] (0.082[c])	—
	<2500	China 6	2020 (2023[d])	WLTP	0.7 (0.5[d])	0.10 (0.05[d])	0.068 (0.035[d])	—	0.06 (0.035[d])	—
	<8500 (lbs)	Tier 3 (bin 1–160)	2017	FTP	0–4.20 (g mi^{-1})	—	—	—	—	0–0.16 (g mi^{-1})

[a] For gas engines only. [b] For passenger cars. [c] For light commercial vehicles. [d] For second stage starting from 2023. WHTC = World Harmonised Transient Cycle. FTP = Federal Test Procedure. WLTP = Worldwide Harmonized Light Vehicles Test Procedure. NEDC = New European Driving Cycle. Data from http://www.transportpolicy.net.

6.[12,13] In view of its worldwide largest market of NGVs, China's policy is expected to promote the development of control technologies for gaseous emissions from NGVs to meet increasingly strict emission limits.

The TWC technology, named after its simultaneous catalytic purification of HC, NO_x and CO, was first applied in gasoline vehicles in the 1970s. To date, it is still the core technology for gaseous emission control of gasoline vehicles.[14,15] For the same purpose, stoichiometric natural gas engines also equip the TWC converter for catalytic purification of their main gaseous pollutants: CH_4, NO_x and CO.[16–21] With the advancement of control technology, the TWC technology has been developed through the following steps: Pt/Rh based TWCs (Ce oxygen storage), high-temperature TWCs (950 °C, Pt/Rh/Pd, Ce–Zr oxygen storage), all palladium (Pd) TWCs (also named Pd-only TWCs, layered coating, Ce–Zr oxygen storage), high-temperature close-coupled TWCs (for low-emission vehicles, 1050 °C, no Ce), and high-temperature close-coupled TWCs (for ultra-low-emission vehicles, larger volume, higher noble metal loading).[22] The major HC of exhaust emissions from NGVs is methane (over 90 vol%), which is a powerful greenhouse gas and harder to oxidize than most HCs.[23,24] Generally, the conversion of methane is less than 15% by conventional TWCs equipped on the NGVs which are retrofitted from gasoline vehicles.[25] To complete the total purification of methane under the same working conditions of engines, more than three-fold loadings of noble metals are needed in comparison to conventional TWCs (up to 0.01 g cm^{-3} against 0.003 g cm^{-3}).[26,27] In addition, the coupling reaction between CH_4 and NO_x is much more difficult than that between non-methane HC (NMHC) and NO_x, which leads to less conversion of NO_x compared with gasoline vehicles. Therefore, it is a great challenge for the control technology of exhaust emissions from NGVs to meet the strict emission limits under the precondition of cost control.

As far as we know, previous review articles were mainly focused on the abatement of methane emissions from NGVs,[10,28,29] while studies on the three-way catalytic applications for NGVs are very limited (Table 3). This paper

 This journal is © The Royal Society of Chemistry 2020

Published on 05 August 2020. Downloaded on 11/17/2020 7:25:32 AM.

Table 3 TWCs for NGVs in previous studies

Catalysts	Preparation methods	Treatment conditions	Reaction conditions	Catalytic activity	Ref.
4.3 wt% Pt–0.48 wt% $Rh/CeO_2–ZrO_2–La_2O_3–Nd_2O_3$	Modified double-solvent	Calcined at 800 °C, 16 h, 10 vol% H_2O, 2 vol% O_2	1000 ppm CH_4, 4800 ppm CO, 960 ppm NO, 3920 ppm O_2, 10 vol% H_2O, 10 vol% CO_2 and bal. N_2, TGFR: 1680 mL min^{-1}, GHSV: 40 000 h^{-1}	T_{90} of CH_4, CO, and NO were 435 °C, 237 °C, and 433 °C, respectively, for aged catalyst	158
1.5 wt% $Pd/CeO_2–ZrO_2–Al_2O_3–La_2O_3$	Co-precipitation and impregnation	Calcined at 550 °C, 2 h, air (fresh)/900 °C, 5 h, air (aged)	0.063 vol% CH_4, 0.063 vol% NO, 0.40 vol% CO, 10 vol% H_2O, 12 vol% CO_2, 0.29 vol% O_2 and bal. N_2, GHSV: 34 000 h^{-1}	T_{50} of CH_4, CO, and NO_x were 345 °C, 144 °C, and 181 °C, T_{90} of CH_4, CO, and NO_x were 417 °C, 178 °C and 228 °C (fresh), respectively; T_{50} of CH_4, CO, and NO_x were 382 °C, 165 °C and 200 °C, T_{90} of CH_4, CO, and NO_x were 445 °C, 200 °C and 255 °C (aged), respectively	137
1.28 wt% Pt–0.14 wt% $Rh/CeO_2–ZrO_2–Y_2O_3–La_2O_3–Al_2O_3$	Co-precipitation and impregnation	550 °C, 3 h, air	0.087 vol% CH_4, 0.40 vol% CO, 0.073 vol% NO, 12.0 vol% CO_2, 10–12 vol% H_2O and bal. N_2, GHSV: 34 000 h^{-1}	T_{50} of CH_4, CO, and NO were 342–440 °C, 114–153 °C, and 149–414 °C, respectively; T_{90} of CH_4, CO, and NO were 398–>500 °C, 179–361 °C, and 174–451 °C, respectively	138
A full-size honeycomb Pd-only commercial TWC (include Al, Ce, Zr)	Incipient wetness	600 °C, 10 h, air	1500 ppm CH_4, 7000 ppm CO, 1600 ppm NO, 5700 ppm O_2, 5 vol% H_2O and bal. N_2, GHSV: 75 000 h^{-1}	T_{50} of CH_4 was 350 °C, T_{90} of CH_4 was above 600 °C, T_{100} of NO was 400 °C, CO conversion was 200–600 °C	33
6 wt% $Pd/La_2O_3–Al_2O_3$ + 10 wt% $CeO_2–ZrO_2$	Impregnation	550 °C, 3 h, air	1035 ppm CH_4, 4960 ppm CO, 930 ppm NO, 10 vol% CO_2, 10 vol% H_2O, 0.3 vol% O_2 and bal. N_2, GHSV: 40 000 h^{-1}	T_{100} of CH_4, CO and NO were around 500 °C simultaneously	36
Pd/Al_2O_3/1.8 wt% $P/Pd/Al_2O_3$ and 7.5 wt% $P/Pd/Al_2O_3$	Impregnation	500 °C, 4 h/700 °C, 5 h (P modified)	1300 ppm CH_4, 7000 ppm CO, 1600 ppm NO, and 7000 ppm O_2 in He, TGFR: 100 mL min^{-1}, GHSV: 7000 h^{-1}	T_{100} of CO and CH_4 increased 50 °C and 120 °C with 1.8 wt% P, respectively; T_{100} of CO and CH_4 increased 114 °C and above 220 °C with 7.5 wt% P, respectively	163
A commercial TWC from a French compact car (Pd, Pt, Rh, Ce, Zr, Ba and Al)	Not reported	Calcined at 500 °C, 2 h, air	1700 ppm CH_4, 4700 ppm CO, 2500 ppm NO, 4800 ppm O_2, 3400 ppm H_2, 9.25 vol% CO_2, 18 vol% H_2O and bal. N_2, GHSV: 40 000 h^{-1}	T_{100} of CO and NO_x were 300 °C and 315 °C, respectively, T_{50} of CH_4 was 277 °C	35
Commercial TWCs from a compact car and a station wagon CNG vehicle (Pd, Pt, Rh, Ce, Zr, Ba, La and Al)	Not reported	Calcined at 500 °C, air	0.25% NO, 0.17% CH_4, 0.48% of O_2, 9.25% CO_2, 0.47% CO, 0.34% H_2 and 18% H_2O, GHSV: 40 000 h^{-1}	T_{50} of CH_4, NO and CO were about 310–375 °C, 280–360 °C, 125–175 °C, respectively	37
3 wt% Pd–15 wt% Ba/alumina	Incipient wetness	Calcined at 550 °C, 3 h, air	400 ppm CH_4, 7000 ppm CO, 500 ppm NO, varied O_2, 800 ppm H_2, 10 vol% CO_2, 6 vol% H_2O and bal. N_2/He, TGFR: 400 mL min^{-1}, GHSV: 50 000 h^{-1}	T_{50} of CH_4, NO and CO were about 352–411 °C, 201 °C, 172–203 °C, respectively	139
1.25 wt% Pd/CeLa/Al	Peptizing and impregnation	Calcined at 550 °C, 3 h, air	0.074 vol% CH_4, 0.076 vol% NO, 0.380 vol% CO, 10 vol% H_2O, 10 vol% CO_2 and bal. N_2, GHSV: 38 000 h^{-1}	T_{50} of CH_4 and CO were 411 °C and 167 °C, respectively; T_{90} of CH_4 and CO were 435 °C and 193 °C, respectively	38

TGFR: total gas flow rate. GHSV: gas hourly space velocity. T_{50}, T_{90} and T_{100}: the temperature of 50%, 90% and 100% reactant conversion, respectively.

Published on 05 August 2020. Downloaded on 11/17/2020 7:25:32 AM.

aims to briefly review the TWC technology of NGVs in particular for Pd-based catalysts, starting from technical fundamentals, to the roles of catalyst components (active phases, supports, and promoters), and then novel preparations of catalysts as well as resistance to thermal and chemical aging will be briefly introduced. Finally, the main challenges and future perspectives of TWCs in the field will be discussed.

2. Fundamentals

2.1 Working windows

The air–fuel ratio (λ) of the engine is closely related to the efficiency of the TWC converter. Under the rich-burn condition ($\lambda < 1$), CO and H_2 remove O* and dissociate NO, but CO and CH_4 are hard to completely oxidize due to the lack of oxygen. Under the lean-burn condition ($\lambda > 1$), sufficient oxygen promotes complete oxidation of CO and CH_4 but inhibits the dissociation of NO.[30] The TWC converts CO, CH_4 and NO_x into CO_2, H_2O and N_2 simultaneously only under stoichiometric conditions ($\lambda = 1$) (Fig. 2). Any small changes in the air–fuel ratio will have a significant impact on the TWC performance. Therefore, keeping the engine working under stoichiometric conditions, *i.e.* TWC working window, is crucial to the purification efficiency of the exhaust emissions.

In addition, the understanding of the catalyst chemistry under the periodic rich-burn and lean-burn conditions is also a crucial issue for the performance of TWCs. Compared with the steady-state operation, the working window of a commercial Pd–Rh/Al_2O_3 catalyst widens under dithering conditions. The number of PdO/Pd^0 active phases is increased by periodically shifting from the rich-burn to the lean-burn conditions with varying oscillation amplitudes, which explains more stable and higher conversions of NO and CH_4.[31–33] The simulation indicates that there is an optimal dithering amplitude to obtain the best result of emission control.[34]

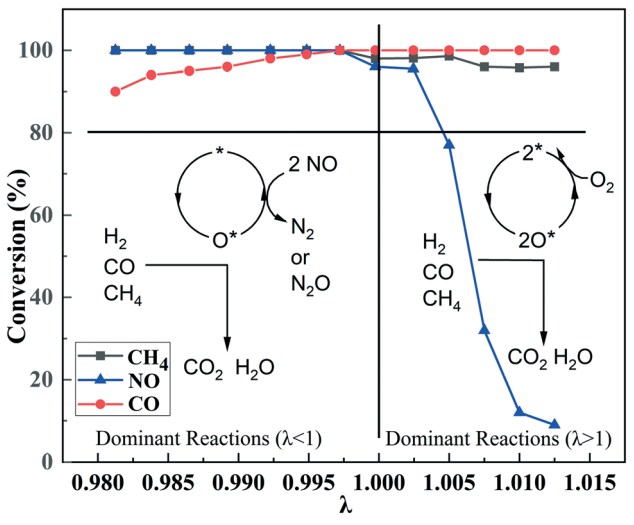

Fig. 2 CH_4, CO and NO conversions of Pd/CZ/La–Al at 500 °C under stoichiometric conditions ($\lambda = 1$),[36] CH_4 1035 ppm, NO 930 ppm, CO 4960 ppm, H_2O 10%, CO_2 10%, varied O_2 content and N_2 (balance), and scheme of TWC reactions (*) present on site.[35] Copyright 2009 and 2017, Elsevier B.V.

2.2 Reaction equations

The key reaction equations of the TWC technology are as follows:[35,36]

Oxidation reactions:

$$H_2 + O_2 \rightarrow H_2O \quad (1)$$

$$CO + O_2 \rightarrow CO_2 \quad (2)$$

$$CH_4 + O_2 \rightarrow CO_2 + H_2O \quad (3)$$

Reduction reactions:

$$NO + H_2 \rightarrow N_2 + H_2O \quad (4)$$

$$NO + CO \rightarrow N_2 + CO_2 \quad (5)$$

$$NO + CH_4 \rightarrow N_2 + CO_2 + H_2O \quad (6)$$

Except for the above redox reactions, water-gas shift and steam reforming also play important roles during the reaction process of TWCs.[35]

Water-gas shift:

$$CO + H_2O \leftrightarrow CO_2 + H_2 \quad (7)$$

Methane steam reforming:

$$CH_4 + H_2O \rightarrow CO + H_2 \quad (8)$$

$$CH_4 + H_2O \rightarrow CO_2 + H_2 \quad (9)$$

Salaün *et al.*[35,37] concluded that CO/O_2 and NO/H_2 were dominant reactions from 100 to 250 °C, and CH_4 started to be oxidized (CH_4/O_2, CH_4/NO) from 250 to 400 °C. Li *et al.*[38] further indicated that CO oxidation (CO/O_2) preferentially preceded the CO/NO reaction which explained that NO conversion decreased when the temperature increased from 180 to 340 °C. At higher temperatures, NO conversion coincided with CH_4 conversion (CH_4/NO) until NO was completely converted. The CH_4/NO reaction was faster than the CH_4/O_2 reaction, and CH_4 oxidation proceeded rapidly after 100% conversion of NO.

3. Catalyst components

3.1 Active components

3.1.1 Noble metals. To date, the Pd-based catalyst has been the most efficient TWC to remove gaseous emissions from NGVs. The noble metals of most commercial TWCs are

 This journal is © The Royal Society of Chemistry 2020

Published on 05 August 2020. Downloaded on 11/17/2020 7:25:32 AM.

composed of Pd and a small amount of Rh and Pt (Fig. 3).[35] Rh is recognized as the most suitable noble metal for NO reduction. It is more active in steam reforming and has better sintering resistance than Pd.[39] Hence, the addition of Rh to Pd-based catalysts helps to improve the thermal stability and reduction performance.[40–43] Both Pd and Pt have excellent oxidizing activities for CH_4 and CO. Pd has excellent three-way catalytic activity with higher hydrothermal stability than Pt, but its sulphur resistance is rather worse.[44] Due to the impressive ability of methane oxidation, Pd-based catalysts are widely used for abatement of exhaust emissions from NGVs,[45] *e.g.*, the Pd-only catalyst without other noble metals exhibits good three-way catalytic activity.[46] The metallic Pd, PdO, and Pd/PdO pairs on the catalyst surfaces have been shown to have different active phases and specific activities for methane oxidation because of their individual structures and surface energy.[47] Although there were still divergences in the oxidation state of the most active species for Pd-based catalysts, PdO is considered more active for methane oxidation than metallic Pd due to the Pd species in PdO form having more active phases.[36,48,49] Pd oxide plays an important role during methane oxidation, particularly below 677 °C,[50] and it is also found to be active for catalysing the reaction up to 900 °C.[51] However, noble metals will be sintered and deactivated at high temperatures, and hence thermal stability is important for noble metal catalysts, which will be discussed in section 5.1.

Due to the high stability of the C–H bond, methane is not easily completely oxidized, and its light-off temperature is higher than that of most HCs. Hence, the purification efficiency and light-off temperature of methane are considered as the key indicators of TWC performance. Most of the previous reports on Pd-based catalysts are focused on the active phases and reaction mechanism studies of methane oxidation.[11,28,49,52–54] The Mars–van Krevelen (MvK) redox mechanism has been proved for the methane oxidation process over PdO:[55,56] PdO provides its lattice oxygen to oxidize methane and is reduced into metallic Pd; PdO is reformed again by the addition of gas-phase oxygen which completes a redox cycle (Fig. 4). The rate-determining step of the MvK mechanism is proposed to be the activation of the first C–H bond.[57,58] On the aspect of the methane oxidation process over metallic Pd, according to the Langmuir–Hinshelwood mechanism, methane and oxygen are both adsorbed on metallic Pd surfaces, and their competitive adsorption determines the rate-determining step.[59] Since metastable intermediate states of metallic Pd and PdO transformation can exist for a long time, which causes surface restructuring and changes in particle size of Pd species, this process needs to be further studied to understand more the reaction mechanisms of methane conversion over Pd-based catalysts.[47,49,60,61]

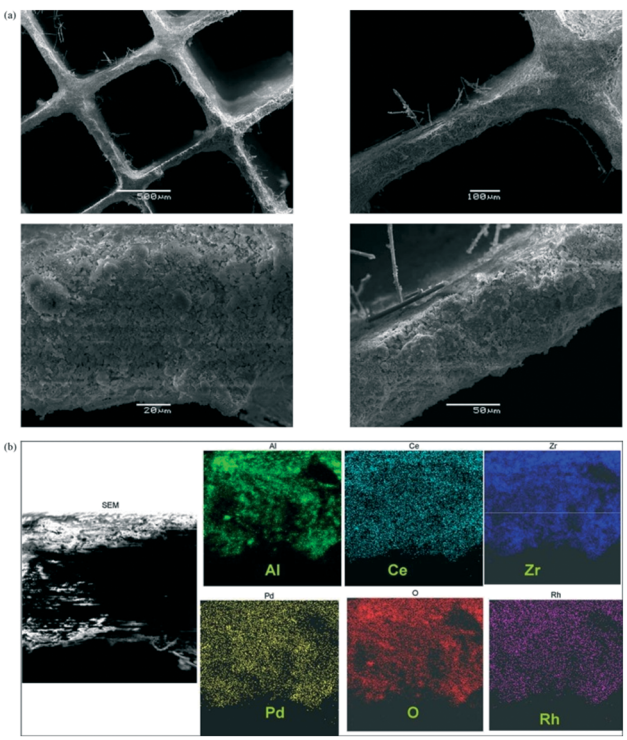

Fig. 3 SEM cartography of fresh NGV converter. (a) General view of the catalyst. (b) EDS cartography.[35] Copyright 2009, Elsevier B.V.

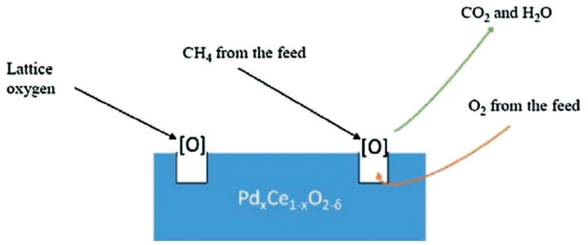

Fig. 4 The proposed MvK mechanism of methane combustion over $Pd_{0.03}Ce_{0.97}O_{2-\delta}$ catalysts.[56] Copyright 2020, Elsevier B.V.

3.1.2 Potential active components. Since the increasing depletion and rising prices of noble metals, noble metal-free oxide catalysts have been developed as an alternative to decrease costs and the environmental hazards of using noble metals.[62,63] The Co_3O_4-based catalyst is one of the representative catalysts, which has a stable spinel-type structure and outstanding catalytic activity for CH_4 and CO oxidation.[64–68] In addition, binary metal oxides formed by Co_3O_4 with additives, *e.g.* Sm, Ce, Zr, Mg, and Al, have better catalytic oxidation of CH_4 and CO.[64,69–72] Spinel-type oxides with a general formula of AB_2O_4 have a stable crystal structure and high thermal stability, which are also considered as a competitive alternative for oxidation catalysts applied for NGVs, *e.g.* $CoCr_2O_4$, $NiCo_2O_4$, $CoAl_2O_4$, $CoFe_2O_4$, $ZnCr_2O_4$, and $CuCo_2O_4$.[73–78] Since both Co and Ni have good activity for methane oxidation and good synergistic effects, $NiCo_2O_4$ exhibits excellent catalytic activity for methane oxidation ($T_{100} < 425$ °C).[79–83] Although these metal oxide catalysts have more stable structures and higher thermal stability than noble metal catalysts, it is still a great challenge to reduce the light-off temperature of methane oxidation

Published on 05 August 2020. Downloaded on 11/17/2020 7:25:32 AM.

without doping noble metals. In addition, more tests are needed under stoichiometric conditions for comprehensive evaluation of their catalytic performance not only for the oxidation of CH_4 and CO but also for the reduction of NO_x.

3.2 Active supports

3.2.1 Aluminas. The main purpose of an active supports, so-called washcoat, is to increase the specific surface area (SSA) of the honeycomb ceramic (or metallic) monolith (*i.e.* the structure supports), which is typically 2 to 4 $m^2\ L^{-1}$, and disperse active phases on the surface of catalysts in order to enhance the catalytic activity (Fig. 5).[84–86] Generally, γ-Al_2O_3 is currently the most widely used support for the TWC converter due to its high SSA, moderate chemical activity, and low cost. Compared to γ-Al_2O_3, other aluminas (α-, θ-, and δ-Al_2O_3) are used for high-temperature close-coupled catalysts due to their high thermal stability above 1000 °C.[86] Among all the common aluminas (θ-, δ-, κ-, η-, and γ-Al_2O_3), PdO supported on θ-Al_2O_3 exhibited the highest methane conversion and thermal stability during methane oxidation.[87] In addition, it is generally accepted that the acid/base property of support oxides would affect the catalytic activity of palladium for methane oxidation, *e.g.* palladium oxide stability[88,89] and oxygen adsorption capacity,[90] particularly at low temperatures.[54] For instance, a combination of $Pd(acetate)_2$ and acetic or propionic acid would enhance the catalytic activity of Pd/Al_2O_3 over methane oxidation.[91] On the other hand, in order to prevent γ-Al_2O_3 changing to low surface area alumina such as α-Al_2O_3 (typically below 10 $m^2\ L^{-1}$) under stoichiometric conditions (up to 1000 °C), various stabilization agents have been employed to enhance its thermal stability, which will be discussed in section 3.3.

3.2.2 Perovskite-type oxides. Perovskite-type oxides with the general formula $ABO_{3\pm\delta}$ have a more stable crystal structure, higher thermal stability and lower cost than noble metal oxides.[92–94] Their distinct self-regenerative property helps to inhibit the agglomeration and growth of active phases on the catalyst surface and keeps good thermal stability.[95,96] By changing the structure of the catalyst (*e.g.* a double-layer configuration containing the active phase in the inner layer), it is able to avoid reaction with sulphur compounds and shows good activity over a wide range of space velocities.[97,98] Hence, perovskites doped with noble metals have been studied as promising alternatives of the current TWCs for stoichiometrically operating NGVs.[99]

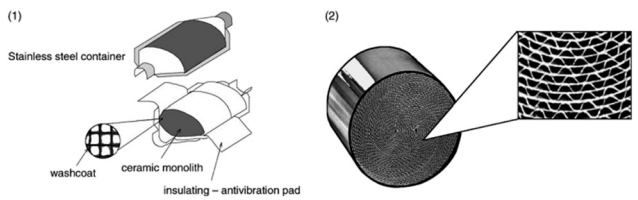

Fig. 5 (1) Diagram of a typical catalytic converter. (2) A metallic honeycomb.[86] Copyright 2003, Elsevier B.V.

Rodríguez *et al.*[100] synthesized two Pd-doped perovskite-based catalysts, Pd–$LaFe_{0.65}Co_{0.35}O_3$ and $LaFe_{0.65}Co_{0.3}Pd_{0.05}O_3$, using a modified citrate route, and tested their NO reduction ability under stoichiometric conditions. The integration of Pd into the perovskite led to higher Pd dispersion in the active state. Compared with the commercial TWC, perovskite-based catalysts produced around 60% less N_2O under stoichiometric conditions. Tzimpilis *et al.*[101,102] prepared Pd-doped perovskite-based catalysts using a combined sol–gel and combustion synthesis method and found that $La_{1.034}Mn_{0.966}Pd_{0.05}O_z$ phases exhibited higher thermal stability and sulphur resistance than the commercial TWC, which could be ascribed to the formation either of mixed La–Pd oxides and/or of a La–Mn double perovskite. In addition, the loading of noble metals used in the perovskite oxides was almost three-fold less than that of the conventional Pd/Al_2O_3 catalysts, which indicated that it could be a competitive candidate for the commercial TWC. Lu *et al.*[103–105] compared a series of A(B, Pd)$O_{3\pm\delta}$ (A = La or Y; B = Mn or Fe) perovskite-based catalysts containing 2 wt% Pd prepared by flame spray synthesis (FSS) under a simulated stoichiometric natural gas mixture at a gas hourly space velocity (GHSV) of 60 000 h^{-1}. Among these catalysts, $Pd/YFeO_{3\pm\delta}$ exhibited the lowest light-off temperature for methane oxidation (T_{50} = 450 °C), which was around 100 °C lower than that of the same catalyst composition gained by the conventional wet-chemical method (Fig. 6). After cycling under reaction conditions up to 850 °C, $Pd/YFeO_{3\pm\delta}$ exhibited identical activity which might be due to the formation of metallic Pd particles and its hexagonal → orthorhombic phase transition. Compared with the commercial TWC, $Pd/YFeO_{3\pm\delta}$ exhibited higher activity after stoichiometric aging (λ = 1, 900 °C) due to the metallic Pd nanoparticles being well-defined in the range of 10–20 nm *versus* most of the thermally aged catalysts with large PdO particles.

3.2.3 Other metal oxides. According to previous reports, single or multiple metal oxides are applied as supports to

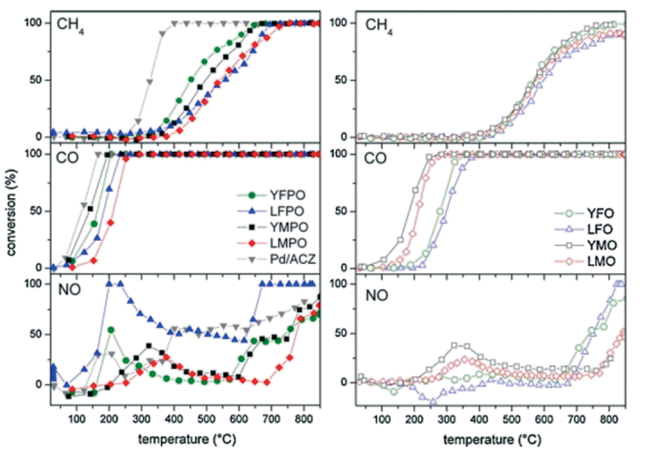

Fig. 6 CH_4, CO and NO conversion profiles of calcined Pd-containing catalysts and Pd/ACZ (left) and Pd-free catalysts (right).[103] Copyright 2014, Elsevier B.V.

 This journal is © The Royal Society of Chemistry 2020

Published on 05 August 2020. Downloaded on 11/17/2020 7:25:32 AM.

improve the catalytic oxidation performance which are mainly focused on either methane oxidation under lean conditions, *e.g.* SiO_2,[106,107] SnO_2,[108,109] CeO_2,[110–112] ZrO_2,[113,114] and Co_3O_4,[72,115] or abatement gas emissions from gasoline engines under stoichiometric conditions, *e.g.* CeO_2–ZrO_2 (ref. 116) and CeO_2–ZrO_2–Al_2O_3.[117,118] In contrast, few studies have been reported on metal oxides used as TWC supports for NGVs. Kalam *et al.*[119] presented a low-cost TWC converter using a wire mesh substrate coated with TiO_2 for its thermal stability above 500 °C and high durability. The SSA for the new support was 25 times higher than that of the original honeycomb ceramic substrate which resulted in the reduction of 24%, 41% and 40% for NO_x, CO and HC emissions, respectively, in comparison to the original TWC converter.

Due to the advantages of the mesoporous framework, mesoporous molecular sieves (MMSs) can provide a mechanism for controlling the metal nanoparticle size and maintain the size during the methane oxidation reaction to avoid metal sintering at elevated temperatures. With high SSA, large specific pore volume, and narrow pore size distribution in comparison to conventional aluminas and zeolites, MMSs are regarded as ideal supports in heterogeneous catalysis for metal oxide catalysts.[120] The performances of SBA-15,[121,122] MCM-41,[123,124] KIT-6 (ref. 125 and 126) and HMS[127,128] have been investigated as support materials of Pd-based catalysts for methane abatement. Hussain *et al.*[126] deposed Pd onto synthesized SBA-15 and KIT-6 mesoporous silica and tested the activity for methane oxidation from exhaust emissions by compressed natural gas (CNG) engines. As confirmed by TEM and STEM, PdO nanoparticles (1–5 nm) were highly dispersed on SBA-15 and KIT-6. As a result, all the catalysts with different Pd loadings (0.25–0.7 wt%) completed 100% methane conversion under 750 °C, particularly for the KIT-6 0.7 wt% Pd catalyst with T_{100} of CH_4 at less than 450 °C. On the other hand, since methane is the main HC of exhaust emissions from NGVs, methane selective catalytic reduction (CH_4-SCR) is an effective method for simultaneous catalytic purification of CH_4 and NO_x by using CH_4 as a reducing agent.[129,130] Mendes *et al.*[131–133] prepared bimetallic PdCe-HMOR catalysts by ion exchange and incipient wetness impregnation to depose Pd and Ce onto HMOR, respectively. As Ce loading above 3 wt%, methane oxidation is strongly enhanced (*ca.* T_{90} = 550 °C), in particular at high temperatures. The optimal Pd/Ce species distribution is gained with 0.3 wt% Pd and 2 wt% Ce, resulting in the best SCR performance.

Overall, more technological improvements and experimental tests are still required towards the commercial application for these catalysts, *e.g.* water resistance at low temperatures and thermal stability at high temperatures. In real conditions, particularly at high space velocities, all these mixed oxide catalysts have not exhibited sufficiently good performances. Their real catalytic activity for the abatement of CH_4, CO and NO_x emitted by CNG engines under stoichiometric conditions is still unclear.

3.3 Promoters

3.3.1 Classic promoters. The promoters for TWCs, particularly for Pd-based catalysts, usually include alkali metals (Mg, Ca, Ba, *etc.*),[134] rare earths (La, Ce, Y, *etc.*)[135] and transition metals (Mn, Fe, Co, Ni, *etc.*).[136] They are aimed to improve the catalytic activity, hydrothermal stability, sulphur resistance ability, *etc.* At present, the main purpose of the TWC improvement is to enhance the catalytic activity of methane oxidation at low temperatures and increase its hydrothermal stability at elevated temperatures. In previous literature, Ce, Zr, Ba, La, Y, and their mixed metal oxides have been reported as the most common promoters to improve the performance of Pd-based catalysts under stoichiometric conditions.[38,137–139]

The most common promoter used in commercial TWCs is CeO_2–ZrO_2 (CZ) composite as a mixed solid-state solution, leading to a better oxygen storage capability (OSC) and higher hydrothermal stability and durability.[140–143] The additive cation (Zr^{4+}) into the CZ lattice contributed to increase the structural defect concentration, improve the oxygen mobility, and enhance the Ce^{3+}/Ce ratio on the surface of Pt–Rh bimetallic catalysts, which produced more oxygen vacancies and cerium in the Ce^{3+} state, thus increasing the NO conversation.[138] The doping of Y^{3+} ions into CZ could enhance lattice oxygen mobility, Ce^{3+} concentration, and oxygen uptake capacity.[144] Using electron spectroscopy to characterize the first layer of the active phases, the percentages of Ce and Zr at the surface of a commercial TWC is roughly 0.84% and 2.44%.[35] Generally, CZ doping can help to maintain the PdO_x state under reaction conditions and enhance the dispersion of Pd/PdO active phase pairs for methane oxidation.[145] Investigating the active sites for methane oxidation close to stoichiometric conditions, this result was further confirmed by *ex situ* XPS. Due to the positive interaction between Pd and CZ, active oxygen mobility from CZ to Pd could promote the stability of PdO species whether under rich or lean conditions with around 64% superficial Pd species in the PdO state (Fig. 7).[36] The

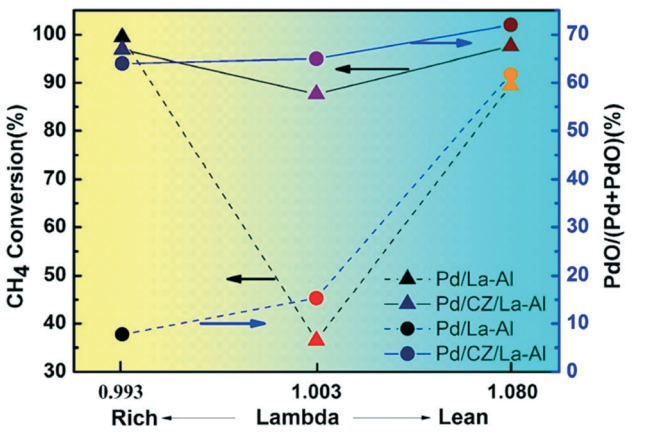

Fig. 7 The ratio of PdO/(Pd + PdO) and CH_4 conversion at different λ values.[36] Copyright 2017, Elsevier B.V.

Published on 05 August 2020. Downloaded on 11/17/2020 7:25:32 AM.

addition of 4 wt% CeO_2 and/or La_2O_3 enhanced the electron density around Pd and promoted Pd dispersion on the surface of Pd/YZ–Al_2O_3 (Y and Zr modified Al_2O_3) catalysts in the increasing order Pd/CeLa/Al > Pd/La/Al > Pd/Ce/Al > Pd/Al. The presence of CeO_2 could facilitate the coupling reaction of NO/CO below 340 °C, which benefited from the redox couple of Ce^{3+}/Ce^{4+}, and the addition of La_2O_3 enhanced the low-temperature activities with the highest NO conversion appearing at around 180 °C.[38]

Ba is also an important promoter which is usually doped in commercial TWCs dedicated to NGV applications.[35] Previous studies reported that Ba had a positive effect on the hydrothermal stability of Pd-based catalysts, which could be more obvious at temperatures over 1000 °C in terms of surface area stabilization.[146,147] Due to the similar electron configuration to Rh, the addition of Ba could help to increase the electron density around Pd(II). This Rh-like catalytic property could enhance TWC performance, particularly for NO_x conversion.[148] Klingstedt *et al.*[139] observed that both fresh and aged Pd–Ba/Al have significantly higher dispersions and smaller mean particle sizes of Pd in comparison to the Pd-only catalyst. The T_{50} of methane oxidation under substoichiometric conditions (λ = 0.99) decreased, and its lambda window was widened after doping of Ba, which resulted in an increased activity both for the fresh and aged (850 °C,16 h) catalysts.

3.3.2 Other potential promoters. The recent improvement in promoters for methane oxidation under the lean-burn condition might be favourable for TWCs. The addition of TiO_2 is able to promote the interaction with PdO and increase the average pore diameter, amount of surface active oxygen, and the electron density around PdO, which improved the oxidation activity of Pd catalysts.[149,150] As an additive, Ni is observed to improve the hydrothermal stability of the support as well as the reducibility of PdO over Pd/ZrO_2–Al_2O_3 catalysts.[151] The modified Pd catalysts with ZnO show good activities at low temperature and high water-resistant performance in methane oxidation.[152,153] The rare earths, *e.g.* Y, Ce, and Pr, are found to be highly effective in improving the structure and enhancing the reduction ability of Pd catalysts. They are able to increase the amounts of surface active oxygen species and the dispersion of Pd particles, consequently enhancing the catalytic performance of methane oxidation.[154]

4. Preparation methods

Basically, TWCs are prepared by co-precipitation and impregnation methods.[155] These approaches are essential to control the physicochemical properties of the catalysts and thus determine the catalytic performance of the emission abatement. However, it is challenging for the two methods to further enhance the catalytic performance, *e.g.*, high dispersion of noble metals, hydrothermal stability, sulphur resistance and water resistance abilities. Hence, recent studies are concentrating on the development of methods for more competitive catalysts applied in the TWC converter of NGVs, which are briefly introduced below. Derived from co-deposition of cerium and cobalt oxides, Soloviev *et al.*[156] observed that the Pd/Co_3O_4/cordierite catalyst had higher oxidation activity of CO and C_6H_{14} in comparison to successive deposition in the three-way catalytic reactions, which was probably caused by better mobility of surface oxygen and higher dispersity of components during the catalytic composition. Shang *et al.*[138] proposed that the co-impregnation method produced large Pt-enriched bimetallic Pt–Rh particles on the surface of Pt–Rh catalysts, thus blocking active Rh sites and decreasing the catalytic activity. Compared to the co-impregnation approach, the Pt–Rh catalyst derived from physical mixing exhibited a homogeneous mixture of Pt and Rh sites on the surface and had synergistic contributions to CH_4, CO, and NO conversions, thus enhancing the three-way activity significantly. Chen *et al.*[157] proposed that the Pt/CeO_2–ZrO_2–La_2O_3–Al_2O_3 TWC prepared by a double-solvent (water and *n*-hexane) approach completed 100% conversion of methane oxidation at 396 °C (GHSV = 34 000 h^{-1}), which was about 46 °C lower in comparison to the incipient wetness impregnation method. In addition, Chen *et al.*[158] modified the double-solvent method with colloidal synthesis and used ethanol as a reducing agent instead of *n*-hexane at the final step for a TWC of Pt–Rh/CeO_2–ZrO_2–La_2O_3–Nd_2O_3. The higher species of Pt^0 and larger concentration of Ce^{3+} were obtained by the modified method, which led to enhancement of the catalytic activity performance of CH_4, CO, and NO by both fresh and aged catalysts, particularly for a 65 °C lower temperature of methane conversion (T_{90}) after hydrothermal aging (800 °C, 16 h). Hu *et al.*[159] developed Pd catalysts *via* a two-step procedure (Fig. 8), *i.e. in situ* reduction process with formaldehyde as a reducing agent before an oxidation step at 550 °C, which slowed down the kinetic growth of both Pd and PdO nanoparticles and generated high dispersion of PdO nanoparticles. Compared to the traditional one-pot method, the two-step preparation method enhanced the catalytic performance of both CH_4 and NO removal from the exhaust emission of NGVs. Using the atomic layer deposition (ALD) method, Onn *et al.*[160] modified porous $MgAl_2O_4$ support by a

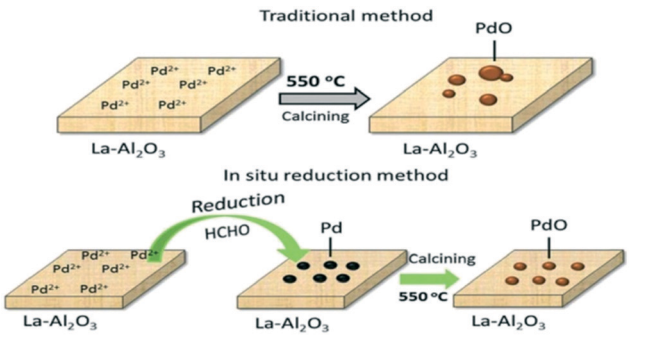

Fig. 8 *In situ* reduction method of Pd^{2+} by formaldehyde.[159] Copyright 2017, Royal Society of Chemistry.

This journal is © The Royal Society of Chemistry 2020

Published on 05 August 2020. Downloaded on 11/17/2020 7:25:32 AM.

$LaFeO_3$ film as a high-surface-area support for Pd, which exhibited more uniform initial Pd distribution and thermal stability than that prepared by a simple impregnation method.

5. Thermal and chemical aging

Similar to gasoline vehicles, thermal and chemical aging also cause catalyst deactivation of NGVs.[161–164] Thermal aging is attributed to long-term exposure at high temperatures under the operating conditions, which would cause sintering of noble metals and supports. Chemical aging of TWCs is due to Mg, P, Zn, Ca, Si, Pb, or S originating from either lubrication oil additives or fuel contaminants, which results in catalyst deactivation by poisoning active phases and suppression of OSC.[165–167]

5.1 Thermal aging

Since the real temperature of exhaust emissions under stoichiometric conditions could be over 1000 °C, the noble metals are easily sintered and aggregated on the supports and become deactivated.[168] After thermal aging by exposing the catalysts in air with 10 vol% H_2O at 980 °C for 4 h, extensive Pd sintering was observed both on Pd–Rh/Al_2O_3 and commercial NGV TWC, which indicated that the interaction between Pd and Rh was suppressed by thermal aging.[40] Thermal aging also changes the surface composition of bimetallic Pd–Rh particles, which causes changing of product distribution from NO dissociation.[43] A number of approaches have been investigated to enhance the thermal stability which can be mainly divided into two types: chemical approaches and physical approaches.[169] The chemical approaches alter the electronic nature and interactions of the active phase or support to enhance inherent resistance, *e.g.* solvothermal method[136] and ALD post-modification.[160,170] The physical approaches change the spatial structures of the active phase and support in order to establish physical barriers, *e.g.* metal-oxide-shell units (*e.g.* Pd@CeO_2)[111,171] and perovskite supports.[101,102] The studies on thermal resistance of TWCs are limited, but extensive reviews on the thermal resistance of methane oxidation can be found in the literature.[49,136,169,172]

5.2 Water poisoning

Water plays an important role throughout the three-way catalytic reaction process. At low temperatures, water usually occupies the active sites and plays an inhibition role in the reactions, which significantly affected the conversions of CH_4, CO and NO. Water can absorb on palladium (Pd^{2+}) and form $Pd(OH)_2$ below 250 °C, which reduces the catalyst activity and inhibits CH_4 oxidation. Water inhibition is also supposed to cause OH group blocking of oxygen exchanges between active sites and supports, thus decreasing catalytic activity.[35,37] In addition, Pd re-oxidation during the cooling ramp in dry feed is also suppressed in the presence of water.[173] However, water adsorption becomes more reversible and its effect decreases with increasing reaction temperature.[174] It participates in the reactions (H_2O/CO, H_2O/CH_4), starting to promote CO and CH_4 conversions by water-gas shift and steam reforming of methane.[35,37] The water inhibition turns to be negligible above 500 °C, while sintering of noble metals and thermal stability becomes more important.[174]

5.3 Sulphur poisoning

Sulphur compounds originating from fuel contaminants are powerful poisoning agents, particularly for Pd-based catalysts even at ppm levels.[44] Recent studies have provided very detailed deactivation mechanisms of Pd-based catalysts by surface-sensitive photo-electron spectroscopy:[49,175,176] at low temperatures (below 450 °C), sulphates are formed close to the active phase by SO_2 oxidation by PdO; at higher temperatures (above 500 °C), PdO becomes more resistant to sulphur poisoning due to sulphur spilling over onto the promoter. Since the active sites are saturated by chemisorbed SO_3 and/or sulphates, the presence of sulphur could strongly deactivate CH_4, CO, and NO conversions. Therefore, promoters are needed to enhance the sulphur resistance of TWCs. The addition of CeO_2 assisted in promoting sulphur resistance due to the formation of stable compounds with SO_x.[156,177] Pd@ZrO_2 catalysts also showed good resistance to SO_2 poisoning due to less sulphate formation, and the presence of sulphates could be removed during regeneration.[176]

5.4 Phosphorus poisoning

Chemical aging with P is another severe poisoning which causes physical and chemical modifications in TWCs, *e.g.*, changing the support by forming $CePO_4$ and $AlPO_4$ phases[178–180] and generating $CePO_4$ to decrease the OSC of $CeZrO_2$.[181,182] The strong cooperation of water and P at 600 °C resulted in aggregation of ceria nanoparticles, incorporation of the Pd active phase and exposure of $CePO_4$ on the catalyst surface.[183] Compared with the three-way catalytic performance of fresh, thermally aged, and chemically aged Pd/Al_2O_3 catalysts under stoichiometric conditions, Matam *et al.*[163] found that P poisoning caused more detrimental physical and chemical modifications to the catalyst. This result confirmed that P poisoning would profoundly deteriorate the three-way catalytic performance of Pd-based catalysts by clogging the support pores, fouling of Pd nanoparticles, and decreasing the reducibility of PdO_x species.

6. Conclusions and perspectives

With the increasingly strict emission limits of NGVs, in particular for CH_4 and NO_x, it is a great challenge for conventional TWCs to meet the requirements of practical applications. As methane is not easily completely oxidized

Published on 05 August 2020. Downloaded on 11/17/2020 7:25:32 AM.

due to the high stability of the C–H bond, its light-off temperature and purification efficiency become the key indicators of the TWC performance of NGVs. Future studies on the reaction mechanisms of methane conversion over Pd-based catalysts are expected to be helpful for enhancing the catalytic activity of methane oxidation, which is still a thriving field of scientific research. On the other hand, the thermal stability and resistance to chemical aging and in particular to water and sulphur poisoning also directly determine the TWC performance of NGVs. More studies are needed to understand the deactivation mechanisms of TWCs under different aging conditions and improve the TWC performance by physical and chemical modifications. In recent studies, perovskite-based catalysts and Co_3O_4-based catalysts have exhibited great potential in the field of TWC development. However, more experiments are still needed to improve their thermal stability and resistance to the poisoning of water, sulphur, and phosphorus over high space velocities for commercial application of NGVs.

To date, the Pd-based catalyst is the most efficient commercial TWC of NGVs, with excellent catalytic purification of gaseous emissions. In order to meet increasingly strict emission limits, noble metals of TWCs cannot be completely replaced yet. In the precondition of guaranteeing the catalyst performance, the reduction of noble metal loadings seems to be the most practical solution at this stage. Transition metals, *e.g.* Co and Ni, which have already shown potential abilities to partly replace noble metals, are reliable to achieve this target. On the other hand, advanced approaches for catalyst synthesis with well-defined nanostructure, *e.g.* solvothermal method, ALD post-modification, and metal-oxide-shell units, are expected to promote the development of new high-performance TWCs with further improved catalytic activity, selectivity, and durability.

Conflicts of interest

All the authors declare that this study involves no conflict of interest.

Acknowledgements

We gratefully acknowledge the financial support from the National Key R&D Program of China (2016YFC0204902), the Strategic Priority Research Program of the Chinese Academy of Sciences (XDA23010200), and the Young Talent Project of the Center for Excellence in Regional Atmospheric Environment, CAS (CERAE201806).

References

1 S. Yeh, *Energy Policy*, 2007, **35**, 5865–5875.
2 M. I. Khan, T. Yasmin and A. Shakoor, *Renewable Sustainable Energy Rev.*, 2015, **51**, 785–797.
3 M. Santhosh Kumar, A. Eyssler, P. Hug, N. van Vegten, A. Baiker, A. Weidenkaff and D. Ferri, *Appl. Catal., B*, 2010, **94**, 77–84.
4 IANGV, http://www.iangv.org, 2018.
5 WOO, http://www.opec.org, 2018.
6 Z. L. Yao, X. Y. Cao, X. B. Shen, Y. Z. Zhang, X. T. Wang and K. B. He, *Atmos. Environ.*, 2014, **94**, 198–204.
7 G. Fontaras, G. Martini, U. Manfredi, A. Marotta, A. Krasenbrink, F. Maffioletti, R. Terenghi and M. Colombo, *Sci. Total Environ.*, 2012, **426**, 65–72.
8 A. Thiruvengadam, M. C. Besch, P. Thiruvengadam, S. Pradhan, D. Carder, H. Kappanna, M. Gautam, A. Oshinuga, H. Hogo and M. Miyasato, *Environ. Sci. Technol.*, 2015, **49**, 5236–5244.
9 M. Vojtisek-Lom, V. Beranek, V. Klir, P. Jindra, M. Pechout and T. Vorisek, *Sci. Total Environ.*, 2018, **616–617**, 774–784.
10 A. Raj, *Johnson Matthey Technol. Rev.*, 2016, **60**, 228–235.
11 P. Gélin and M. Primet, *Appl. Catal., B*, 2002, **39**, 1–37.
12 S. J. Zhang, Y. Wu, X. M. Wu, M. L. Li, Y. S. Ge, B. Liang, Y. Y. Xu, Y. Zhou, H. Liu, L. X. Fu and J. M. Hao, *Atmos. Environ.*, 2014, **89**, 216–229.
13 Y. Wu, S. Zhang, J. Hao, H. Liu, X. Wu, J. Hu, M. P. Walsh, T. J. Wallington, K. M. Zhang and S. Stevanovic, *Sci. Total Environ.*, 2017, **574**, 332–349.
14 M. V. Twigg, *Platinum Met. Rev.*, 1999, **43**, 168–171.
15 M. Shelef and R. W. McCabe, *Catal. Today*, 2000, **62**, 35–50.
16 M. Aslam, H. Masjuki, M. Kalam, H. Abdesselam, T. Mahlia and M. Amalina, *Fuel*, 2006, **85**, 717–724.
17 M. I. Jahirul, H. H. Masjuki, R. Saidur, M. A. Kalam, M. H. Jayed and M. A. Wazed, *Appl. Therm. Eng.*, 2010, **30**, 2219–2226.
18 C. Jang and J. Lee, *Proc. Inst. Mech. Eng., Part D*, 2005, **219**, 825–831.
19 L. Turrio-Baldassarri, C. L. Battistelli, L. Conti, R. Crebelli, B. De Berardis, A. L. Iamiceli, M. Gambino and S. Iannaccone, *Sci. Total Environ.*, 2006, **355**, 64–77.
20 T. F. Yusaf, D. R. Buttsworth, K. H. Saleh and B. F. Yousif, *Appl. Energy*, 2010, **87**, 1661–1669.
21 L. J. Wei and P. Geng, *Fuel Process. Technol.*, 2016, **142**, 264–278.
22 R. M. Heck and R. J. Farrauto, *Appl. Catal., A*, 2001, **221**, 443–457.
23 F. Klingstedt, A. K. Neyestanaki, R. Byggningsbacka, L. E. Lindfors, M. Lundén, M. Petersson, P. Tengström, T. Ollonqvist and J. Väyrynen, *Appl. Catal., A*, 2001, **209**, 301–316.
24 T. V. Choudhary, S. Banerjee and V. R. Choudhary, *Appl. Catal., A*, 2002, **234**, 1–23.
25 S. Oh, *J. Catal.*, 1991, **132**, 287–301.
26 R. J. Farrauto and R. M. Heck, *Catal. Today*, 1999, **51**, 351–360.
27 L. F. Liotta, G. Di Carlo, G. Pantaleo, A. M. Venezia and G. Deganello, *Appl. Catal., B*, 2006, **66**, 217–227.
28 J. Chen, H. Arandiyan, X. Gao and J. Li, *Catal. Surv. Asia*, 2015, **19**, 140–171.
29 M. Kumar, G. Rattan and R. Prasad, *Can. Chem. Trans.*, 2015, **3**, 381–409.
30 F. Zeng and K. L. Hohn, *Appl. Catal., B*, 2016, **182**, 570–579.
31 D. Bounechada, G. Groppi, P. Forzatti, K. Kallinen and T. Kinnunen, *Appl. Catal., B*, 2012, **119**, 91–99.

 This journal is © The Royal Society of Chemistry 2020

Published on 05 August 2020. Downloaded on 11/17/2020 7:25:32 AM.

32 D. Bounechada, G. Groppi, P. Forzatti, K. Kallinen and T. Kinnunen, *Top. Catal.*, 2013, **56**, 372–377.
33 D. Ferri, M. Elsener and O. Kröcher, *Appl. Catal., B*, 2018, **220**, 67–77.
34 F. Zeng, J. Finke, D. Olsen, A. White and K. L. Hohn, *Chem. Eng. J.*, 2018, **352**, 389–404.
35 M. Salaün, A. Kouakou, S. Da Costa and P. Da Costa, *Appl. Catal., B*, 2009, **88**, 386–397.
36 F. J. Huang, J. J. Chen, W. Hu, G. X. Li, Y. Wu, S. D. Yuan, L. Zhong and Y. Q. Chen, *Appl. Catal., B*, 2017, **219**, 73–81.
37 M. Salaün, S. Capela, S. Da Costa, L. Gagnepain and P. Da Costa, *Top. Catal.*, 2009, **52**, 1972–1976.
38 Y. L. Li, X. Y. Zhang, E. Y. Long, H. M. Li, D. D. Wu, L. Cai, M. C. Gong and Y. Q. Chen, *J. Nat. Gas Chem.*, 2009, **18**, 415–420.
39 T. Maillet, J. Barbier, P. Gelin, H. Praliaud and D. Duprez, *J. Catal.*, 2001, **202**, 367–378.
40 Y. Renème, F. Dhainaut, M. Trentesaux, B. Ravanbakhsh, P. Granger, C. Dujardin, L. Gengembre and P. L. De Cola, *Surf. Interface Anal.*, 2010, **42**, 530–535.
41 Y. Renème, F. Dhainaut and P. Granger, *Appl. Catal., B*, 2012, **111–112**, 424–432.
42 Y. Renème, F. Dhainaut, Y. Schuurman, C. Mirodatos and P. Granger, *Appl. Catal., B*, 2014, **160–161**, 390–399.
43 P. Granger, Y. Renème, F. Dhainaut, Y. Schuurman and C. Mirodatos, *Top. Catal.*, 2017, **60**, 289–294.
44 V. Meeyoo, *Appl. Catal., B*, 1998, **16**, L101–L104.
45 G. Centi, *J. Mol. Catal. A: Chem.*, 2001, **173**, 287–312.
46 Z. Hu, C. Z. Wan, Y. K. Lui, J. Dettling and J. J. Steger, *Catal. Today*, 1996, **30**, 83–89.
47 A. K. Datye, J. Bravo, T. R. Nelson, P. Atanasova, M. Lyubovsky and L. Pfefferle, *Appl. Catal., A*, 2000, **198**, 179–196.
48 R. Marques, S. Capela, S. Dacosta, F. Delacroix, G. Djegamariadassou and P. Dacosta, *Catal. Commun.*, 2008, **9**, 1704–1708.
49 M. Monai, T. Montini, R. J. Gorte and P. Fornasiero, *Eur. J. Inorg. Chem.*, 2018, 2884–2893.
50 S. K. Matam, M. H. Aguirre, A. Weidenkaff and D. Ferri, *J. Phys. Chem. C*, 2010, **114**, 9439–9443.
51 J. D. Grunwaldt, N. van Vegten and A. Baiker, *Chem. Commun.*, 2007, 4635–4637.
52 D. Ciuparu, M. R. Lyubovsky, E. Altman, L. D. Pfefferle and A. Datye, *Catal. Rev.: Sci. Eng.*, 2002, **44**, 593–649.
53 L. He, Y. Fan, J. Bellettre, J. Yue and L. Luo, *Renewable Sustainable Energy Rev.*, 2020, **119**, 109589.
54 H. Yoshida, T. Nakajima, Y. Yazawa and T. Hattori, *Appl. Catal., B*, 2007, **71**, 70–79.
55 P. Mars and D. W. van Krevelen, *Chem. Eng. Sci.*, 1954, **3**, 41–59.
56 T. P. O. Mkhwanazi, M. D. Farahani, A. S. Mahomed, S. Singh and H. B. Friedrich, *Appl. Catal., B*, 2020, **275**, 119118.
57 R. E. Hayes, S. T. Kolaczkowski, P. K. C. Li and S. Awdry, *Chem. Eng. Sci.*, 2001, **56**, 4815–4835.
58 R. Burch, D. J. Crittle and M. J. Hayes, *Catal. Today*, 1999, **47**, 229–234.
59 M. Rotko, A. Machocki and B. Stasinska, *Appl. Surf. Sci.*, 2010, **256**, 5585–5589.
60 J. B. Miller and M. Malatpure, *Appl. Catal., A*, 2015, **495**, 54–62.
61 S. K. Matam, G. L. Chiarello, Y. Lu, A. Weidenkaff and D. Ferri, *Top. Catal.*, 2013, **56**, 239–242.
62 J. Kielhorn, C. Melber, D. Keller and I. Mangelsdorf, *Int. J. Hyg. Environ. Health*, 2002, **205**, 417–432.
63 R. Merget and G. Rosner, *Sci. Total Environ.*, 2001, **270**, 165–173.
64 X. L. Xu, H. Han, J. J. Liu, W. M. Liu, W. L. Li and X. Wang, *J. Rare Earths*, 2014, **32**, 159–169.
65 Z. Chen, S. Wang, Y. Ding, L. Zhang, L. Lv, M. Wang and S. Wang, *Appl. Catal., A*, 2017, **532**, 95–104.
66 N. T. Yang, S. L. Ni, Y. H. Sun and Y. Zhu, *Mol. Catal.*, 2018, **452**, 28–35.
67 Z. Y. Pu, H. Zhou, Y. F. Zheng, W. Z. Huang and X. N. Li, *Appl. Surf. Sci.*, 2017, **410**, 14–21.
68 L. Hu, Q. Peng and Y. Li, *J. Am. Chem. Soc.*, 2008, **130**, 16136–16137.
69 A. Choya, B. de Rivas, J. R. González-Velasco, J. I. Gutiérrez-Ortiz and R. López-Fonseca, *Appl. Catal., B*, 2018, **237**, 844–854.
70 Z. Y. Pu, Y. Liu, H. Zhou, W. Z. Huang, Y. F. Zheng and X. N. Li, *Appl. Surf. Sci.*, 2017, **422**, 85–93.
71 T. Xiao, S. Ji, H. Wang, K. S. Coleman and M. L. H. Green, *J. Mol. Catal. A: Chem.*, 2001, **175**, 111–123.
72 L. F. Liotta, H. Wu, G. Pantaleo and A. M. Venezia, *Catal. Sci. Technol.*, 2013, 3.
73 D. Fino, N. Russo, G. Saracco and V. Specchia, *Catal. Today*, 2006, **117**, 559–563.
74 Y. Mahara, T. Tojo, K. Murata, J. Ohyama and A. Satsuma, *RSC Adv.*, 2017, **7**, 34530–34537.
75 X. Y. Li, Y. X. Liu, J. G. Deng, S. H. Xie, X. T. Zhao, Y. Zhang, K. F. Zhang, H. Arandiyan, G. S. Guo and H. X. Dai, *Appl. Surf. Sci.*, 2017, **403**, 590–600.
76 W. Huang, W. W. Zha, D. L. Zhao and S. J. Feng, *Solid State Sci.*, 2019, **87**, 49–52.
77 B. Ivanov, I. Spassova, M. Milanova, G. Tyuliev and M. Khristova, *J. Rare Earths*, 2015, **33**, 382–390.
78 S. Trivedi and R. Prasad, *J. Environ. Sci.*, 2018, **65**, 62–71.
79 S. Trivedi, R. Prasad and S. K. Gautam, *AIChE J.*, 2018, **64**, 2632–2646.
80 Z. S. Zhang, J. W. Li, T. Yi, L. W. Sun, Y. B. Zhang, X. F. Hu, W. H. Cui and X. G. Yang, *Chin. J. Catal.*, 2018, **39**, 1228–1239.
81 S. Trivedi and R. Prasad, *Can. J. Chem. Eng.*, 2018, **96**, 1352–1359.
82 S. Trivedi and R. Prasad, *New J. Chem.*, 2018, **42**, 4142–4154.
83 T. H. Lim, S. J. Cho, H. S. Yang, M. H. Engelhard and D. H. Kim, *Appl. Catal., A*, 2015, **505**, 62–69.
84 P. J. Jodłowski, R. Gołąb, J. Kryca, A. Kołodziej, M. Iwaniszyn, S. T. Kolaczkowski and J. Łojewska, *Top. Catal.*, 2013, **56**, 390–396.
85 P. Dimopoulos Eggenschwiler, D. N. Tsinoglou, J. Seyfert, C. Bach, U. Vogt and M. Gorbar, *Exp. Fluids*, 2009, **47**, 209–222.

Published on 05 August 2020. Downloaded on 11/17/2020 7:25:32 AM.

86 J. Kašpar, P. Fornasiero and N. Hickey, *Catal. Today*, 2003, **77**, 419–449.
87 J. H. Park, J. H. Ahn, H. I. Sim, G. Seo, H. S. Han and C. H. Shin, *Catal. Commun.*, 2014, **56**, 157–163.
88 R. J. Farrauto, J. K. Lampert, M. C. Hobson and E. M. Waterman, *Appl. Catal., B*, 1995, **6**, 263–270.
89 K. Muto, N. Katada and M. Niwa, *Appl. Catal., A*, 1996, **134**, 203–215.
90 C. Cullis, *J. Catal.*, 1983, **83**, 267–285.
91 N. M. Kinnunen, M. Suvanto, M. A. Moreno, A. Savimäki, K. Kallinen, T. J. J. Kinnunen and T. A. Pakkanen, *Appl. Catal., A*, 2009, **370**, 78–87.
92 S. Keav, S. Matam, D. Ferri and A. Weidenkaff, *Catalysts*, 2014, **4**, 226–255.
93 S. Royer, D. Duprez, F. Can, X. Courtois, C. Batiot-Dupeyrat, S. Laassiri and H. Alamdari, *Chem. Rev.*, 2014, **114**, 10292–10368.
94 H. He, H. X. Dai and C. T. Au, *Appl. Catal., B*, 2001, **33**, 65–80.
95 M. Uenishi, H. Tanaka, M. Taniguchi, I. Tan, Y. Sakamoto, S.-i. Matsunaga, K. Yokota and T. Kobayashi, *Appl. Catal., A*, 2005, **296**, 114–119.
96 M. Uenishi, M. Taniguchi, H. Tanaka, M. Kimura, Y. Nishihata, J. Mizuki and T. Kobayashi, *Appl. Catal., B*, 2005, **57**, 267–273.
97 H. Tanaka, *Catal. Surv. Asia*, 2005, **9**, 63–74.
98 T. Muroi, N. Nojiri and T. Deguchi, *Appl. Catal., A*, 2010, **389**, 27–45.
99 D. Fino, N. Russo, G. Saracco and V. Specchia, *Prog. Solid State Chem.*, 2007, **35**, 501–511.
100 G. C. M. Rodríguez, K. Kelm, S. Heikens, W. Grünert and B. Saruhan, *Catal. Today*, 2012, **184**, 184–191.
101 E. Tzimpilis, N. Moschoudis, M. Stoukides and P. Bekiaroglou, *Appl. Catal., B*, 2008, **84**, 607–615.
102 E. Tzimpilis, N. Moschoudis, M. Stoukides and P. Bekiaroglou, *Appl. Catal., B*, 2009, **87**, 9–17.
103 Y. Lu, K. A. Michalow, S. K. Matam, A. Winkler, A. E. Maegli, S. Yoon, A. Heel, A. Weidenkaff and D. Ferri, *Appl. Catal., B*, 2014, **144**, 631–643.
104 Y. Lu, S. Keav, V. Marchionni, G. L. Chiarello, A. Pappacena, M. Di Michiel, M. A. Newton, A. Weidenkaff and D. Ferri, *Catal. Sci. Technol.*, 2014, **4**, 2919–2931.
105 Y. Lu, S. Keav, A. E. Maegli, A. Weidenkaff and D. Ferri, *Top. Catal.*, 2015, **58**, 910–918.
106 B. Li, H. Li, W. Z. Weng, Q. Zhang, C. J. Huang and H. L. Wan, *Fuel*, 2013, **103**, 1032–1038.
107 D. Pi, W. Z. Li, Q. Z. Lin, Q. F. Huang, H. Q. Hu and C. Y. Shao, *Energy Technol.*, 2016, **4**, 943–949.
108 K. Sekizawa, H. Widjaja, S. Maeda, Y. Ozawa and K. Eguchi, *Appl. Catal., A*, 2000, **200**, 211–217.
109 Z. Y. Zhao, B. W. Wang, J. Ma, W. C. Zhan, L. Wang, Y. L. Guo, Y. Guo and G. Z. Lu, *Chin. J. Catal.*, 2017, **38**, 1322–1329.
110 M. Hoffmann, S. Kreft, G. Georgi, G. Fulda, M.-M. Pohl, D. Seeburg, C. Berger-Karin, E. V. Kondratenko and S. Wohlrab, *Appl. Catal., B*, 2015, **179**, 313–320.
111 M. Cargnello, J. J. Delgado Jaen, J. C. Hernandez Garrido, K. Bakhmutsky, T. Montini, J. J. Calvino Gamez, R. J. Gorte and P. Fornasiero, *Science*, 2012, **337**, 713–717.
112 J. Ma, Y. Lou, Y. F. Cai, Z. Y. Zhao, L. Wang, W. C. Zhan, Y. L. Guo and Y. Guo, *Catal. Sci. Technol.*, 2018, **8**, 2567–2577.
113 Y. Wu, J. J. Chen, W. Hu, K. Zhao, P. F. Qu, P. Q. Shen, M. Zhao, L. Zhong and Y. Q. Chen, *J. Catal.*, 2019, **377**, 565–576.
114 E. P. Hong, C. S. Kim, D. H. Lim, H. J. Cho and C. H. Shin, *Appl. Catal., B*, 2018, **232**, 544–552.
115 G. Ercolino, P. Stelmachowski and S. Specchia, *Ind. Eng. Chem. Res.*, 2017, **56**, 6625–6636.
116 B. Zhao, G. F. Li, C. H. Ge, Q. Y. Wang and R. X. Zhou, *Appl. Catal., B*, 2010, **96**, 338–349.
117 N. Peng, J. F. Zhou, S. H. Chen, X. C. Luo, Y. Q. Chen and M. C. Gong, *J. Rare Earths*, 2012, **30**, 342–349.
118 L. Lan, S. H. Chen, Y. Cao, S. N. Wang, Q. F. Wu, Y. Zhou, M. L. Huang, M. C. Gong and Y. Q. Chen, *J. Mol. Catal. A: Chem.*, 2015, **410**, 100–109.
119 M. A. Kalam, H. H. Masjuki, M. Redzuan, T. M. I. Mahlia, M. A. Fuad, M. Mohibah, K. H. Halim, A. Ishak, M. Khair, A. Shahrir and A. Yusoff, *Sadhana*, 2009, **34**, 467–481.
120 D. Trong On, D. Desplantier-Giscard, C. Danumah and S. Kaliaguine, *Appl. Catal., A*, 2001, **222**, 299–357.
121 M. Boutros, M. E. Gálvez, T. Onfroy and P. Da Costa, *Microporous Mesoporous Mater.*, 2014, **183**, 1–8.
122 J. Bassil, A. AlBarazi, P. Da Costa and M. Boutros, *Catal. Today*, 2011, **176**, 36–40.
123 S. Zribi, B. Albela, L. Bonneviot and M. S. Zina, *Appl. Catal., A*, 2015, **502**, 195–203.
124 I. B. Saïd, K. Sadouki, S. Masse, T. Coradin, L. S. Smiri and S. Fessi, *Microporous Mesoporous Mater.*, 2018, **260**, 93–101.
125 M. Filip, S. Todorova, M. Shopska, M. Ciobanu, F. Papa, S. Somacescu, C. Munteanu and V. Parvulescu, *Catal. Today*, 2018, **306**, 138–144.
126 M. Hussain, F. A. Deorsola, N. Russo, D. Fino and R. Pirone, *Fuel*, 2015, **149**, 2–7.
127 A. M. Venezia, G. Di Carlo, L. F. Liotta, G. Pantaleo and M. Kantcheva, *Appl. Catal., B*, 2011, **106**, 529–539.
128 I. Yuranov, P. Moeckli, E. Suvorova, P. Buffat, L. Kiwi-Minsker and A. Renken, *J. Mol. Catal. A: Chem.*, 2003, **192**, 239–251.
129 J. N. Armor, *Catal. Today*, 1995, **26**, 147–158.
130 Y. J. Li and J. N. Armor, *Appl. Catal., B*, 1992, **1**, L31–L40.
131 A. N. Mendes, V. L. Zholobenko, F. Thibault-Starzyk, P. D. Costa and C. Henriques, *Appl. Catal., B*, 2016, **195**, 121–131.
132 A. Mendes, M. Ribeiro, C. Henriques and P. Da Costa, *Catalysts*, 2015, **5**, 1815–1830.
133 A. N. Mendes, V. Lauga, S. Capela, M. F. Ribeiro, P. Da Costa and C. Henriques, *Top. Catal.*, 2016, **59**, 982–986.
134 X. Auvray, A. Lindholm, M. Milh and L. Olsson, *Catal. Today*, 2018, **299**, 212–218.
135 S. Colussi, A. Trovarelli, C. Cristiani, L. Lietti and G. Groppi, *Catal. Today*, 2012, **180**, 124–130.

 This journal is © The Royal Society of Chemistry 2020

Published on 05 August 2020. Downloaded on 11/17/2020 7:25:32 AM.

136 J. J. Willis, E. D. Goodman, L. Wu, A. R. Riscoe, P. Martins, C. J. Tassone and M. Cargnello, *J. Am. Chem. Soc.*, 2017, **139**, 11989–11997.
137 X. Y. Zhang, E. Y. Long, Y. L. Li, J. X. Guo, L. J. Zhang, M. C. Gong, M. H. Wang and Y. Q. Chen, *J. Nat. Gas Chem.*, 2009, **18**, 139–144.
138 H. Y. Shang, Y. Wang, Y. J. Cui, R. M. Fang, W. Hu, M. C. Gong and Y. Q. Chen, *Chin. J. Catal.*, 2015, **36**, 290–298.
139 F. Klingstedt, H. Karhu, A. K. Neyestanaki, L. E. Lindfors, T. Salmi and J. Väyrynen, *J. Catal.*, 2002, **206**, 248–262.
140 M. Alifanti, B. Baps, N. Blangenois, J. Naud, P. Grange and B. Delmon, *Chem. Mater.*, 2003, **15**, 395–403.
141 L. F. Liotta, A. Macaluso, A. Longo, G. Pantaleo, A. Martorana and G. Deganello, *Appl. Catal., A*, 2003, **240**, 295–307.
142 A. I. Kozlov, D. H. Kim, A. Yezerets, P. Andersen, H. H. Kung and M. C. Kung, *J. Catal.*, 2002, **209**, 417–426.
143 H. He, H. X. Dai, L. H. Ng, K. W. Wong and C. T. Au, *J. Catal.*, 2002, **206**, 1–13.
144 H. He, H. X. Dai, K. W. Wong and C. T. Au, *Appl. Catal., A*, 2003, **251**, 61–74.
145 K. Fujimoto, F. H. Ribeiro, M. Avalos-Borja and E. Iglesia, *J. Catal.*, 1998, **179**, 431–442.
146 M. Machida, K. Eguchi and H. Arai, *J. Catal.*, 1987, **103**, 385–393.
147 M. Johnson, *J. Catal.*, 1990, **123**, 245–259.
148 T. Kobayashi, T. Yamada and K. Kayano, *Appl. Catal., B*, 2001, **30**, 287–292.
149 X. Y. Zhang, E. Y. Long, Y. L. Li, L. J. Zhang, J. X. Guo, M. C. Gong and Y. Q. Chen, *J. Mol. Catal. A: Chem.*, 2009, **308**, 73–78.
150 Y. Wang, H. D. Xu, H. Y. Shang, M. C. Gong and Y. Q. Chen, *J. Energy Chem.*, 2014, **23**, 461–467.
151 Y. Wu, G. X. Li, W. Hu, F. J. Huang, J. J. Chen, L. Zhong and Y. Q. Chen, *J. Taiwan Inst. Chem. Eng.*, 2018, **85**, 176–185.
152 H. Y. Shang, Y. Wang, M. C. Gong and Y. Q. Chen, *J. Nat. Gas Chem.*, 2012, **21**, 393–399.
153 Y. Wang, H. Y. Shang, H. D. Xu, M. C. Gong and Y. Q. Chen, *Chin. J. Catal.*, 2014, **35**, 1157–1165.
154 H. X. Liu, B. W. Zhao, Y. S. Chen, C. J. Ren and Y. Q. Chen, *J. Rare Earths*, 2017, **35**, 1077–1082.
155 P. Munnik, P. E. de Jongh and K. P. de Jong, *Chem. Rev.*, 2015, **115**, 6687–6718.
156 S. O. Soloviev, P. I. Kyriienko and N. O. Popovych, *J. Environ. Sci.*, 2012, **24**, 1327–1333.
157 J. J. Chen, F. J. Huang, W. Hu, G. X. Li, L. Zhong and Y. Q. Chen, *RSC Adv.*, 2016, **6**, 40366–40370.
158 J. J. Chen, W. Hu, F. J. Huang, G. X. Li, S. D. Yuan, M. C. Gong, L. Zhong and Y. Q. Chen, *J. Rare Earths*, 2017, **35**, 857–866.
159 W. Hu, G. X. Li, J. J. Chen, F. J. Huang, Y. Wu, S. D. Yuan, L. Zhong and Y. Q. Chen, *Chem. Commun.*, 2017, **53**, 6160–6163.
160 T. M. Onn, M. Monai, S. Dai, E. Fonda, T. Montini, X. Pan, G. W. Graham, P. Fornasiero and R. J. Gorte, *J. Am. Chem. Soc.*, 2018, **140**, 4841–4848.
161 L. Martín, *Appl. Catal., B*, 2003, **44**, 41–52.
162 A. Winkler, P. Dimopoulos, R. Hauert, C. Bach and M. Aguirre, *Appl. Catal., B*, 2008, **84**, 162–169.
163 S. K. Matam, E. H. Otal, M. H. Aguirre, A. Winkler, A. Ulrich, D. Rentsch, A. Weidenkaff and D. Ferri, *Catal. Today*, 2012, **184**, 237–244.
164 T. Kanerva, M. Honkanen, T. Kolli, O. Heikkinen, K. Kallinen, T. Saarinen, J. Lahtinen, E. Olsson, R. L. Keiski and M. Vippola, *Catalysts*, 2019, **9**, 137–152.
165 A. Winkler, A. Eyssler, A. Mägli, A. Liati, P. Dimopoulos Eggenschwiler and C. Bach, *Fuel*, 2013, **111**, 855–864.
166 T. Tabata, K. Baba and H. Kawashima, *Appl. Catal., B*, 1995, **7**, 19–32.
167 S. Y. Christou, M. C. Álvarez-Galván, J. L. G. Fierro and A. M. Efstathiou, *Appl. Catal., B*, 2011, **106**, 103–113.
168 H. Yao, *J. Catal.*, 1977, **50**, 407–418.
169 E. D. Goodman, J. A. Schwalbe and M. Cargnello, *ACS Catal.*, 2017, **7**, 7156–7173.
170 T. M. Onn, M. Monai, S. Dai, L. Arroyo-Ramirez, S. Zhang, X. Pan, G. W. Graham, P. Fornasiero and R. J. Gorte, *Appl. Catal., A*, 2017, **534**, 70–77.
171 G. H. Cai, W. Luo, Y. H. Xiao, Y. Zheng, F. L. Zhong, Y. Y. Zhan and L. L. Jiang, *ACS Omega*, 2018, **3**, 16769–16776.
172 L. De Rogatis, M. Cargnello, V. Gombac, B. Lorenzut, T. Montini and P. Fornasiero, *ChemSusChem*, 2010, **3**, 24–42.
173 O. Mihai, G. Smedler, U. Nylén, M. Olofsson and L. Olsson, *Catal. Sci. Technol.*, 2017, **7**, 3084–3096.
174 R. Gholami, M. Alyani and K. Smith, *Catalysts*, 2015, **5**, 561–594.
175 M. S. Wilburn and W. S. Epling, *Appl. Catal., B*, 2017, **206**, 589–598.
176 M. Monai, T. Montini, M. Melchionna, T. Duchoň, P. Kúš, C. Chen, N. Tsud, L. Nasi, K. C. Prince, K. Veltruská, V. Matolín, M. M. Khader, R. J. Gorte and P. Fornasiero, *Appl. Catal., B*, 2017, **202**, 72–83.
177 L. F. Liotta, G. Di Carlo, G. Pantaleo, A. M. Venezia, G. Deganello, E. Merlone Borla and M. Pidria, *Appl. Catal., B*, 2007, **75**, 182–188.
178 M. J. Rokosz, A. E. Chen, C. K. Lowe-Ma, A. V. Kucherov, D. Benson, M. C. Paputa Peck and R. W. McCabe, *Appl. Catal., B*, 2001, **33**, 205–215.
179 L. Xu, G. Guo, D. Uy, A. E. O'Neill, W. H. Weber, M. J. Rokosz and R. W. McCabe, *Appl. Catal., B*, 2004, **50**, 113–125.
180 M. Kärkkäinen, T. Kolli, M. Honkanen, O. Heikkinen, A. Väliheikki, M. Huuhtanen, K. Kallinen, J. Lahtinen, M. Vippola and R. L. Keiski, *Top. Catal.*, 2016, **59**, 1044–1048.
181 C. Larese, F. C. Galisteo, M. L. Granados, R. Mariscal, J. L. G. Fierro, M. Furió and R. F. Ruiz, *Appl. Catal., B*, 2003, **40**, 305–317.
182 M. López Granados, C. Larese, F. Cabello Galisteo, R. Mariscal, J. L. G. Fierro, R. Fernández-Ruíz, R. Sanguino and M. Luna, *Catal. Today*, 2005, **107–108**, 77–85.
183 M. Monai, T. Montini, M. Melchionna, T. Duchoň, P. Kúš, N. Tsud, K. C. Prince, V. Matolin, R. J. Gorte and P. Fornasiero, *Appl. Catal., B*, 2016, **197**, 271–279.